Revised assignments of the v4=1 vibrational level of CH35Cl3: The ν4 and ν4-ν3 rovibrational bands with remarkable clustering effects

Adina Ceausu-Velcescu, Laurent Manceron, Helmut Beckers, Pierre Ghesquiere, Petr Pracna

Revised assignments of the ν_4=1 vibrational level of $CH^{35}Cl_3$: The ν_4 and ν_4-ν_3 rovibrational bands with remarkable clustering effects

Adina CEAUSU – VELCESCU [a], Laurent MANCERON [b,c], Helmut BECKERS [d], Pierre GHESQUIERE [e], Petr PRACNA [f]

[a] *Université de Perpignan, LAMPS, 52 Avenue Paul Alduy, 66860 Perpignan Cedex, France*
[b] *Ligne AILES, Synchrotron SOLEIL, L'Orme des Merisiers, St-Aubin BP48, 91192 Gif-sur-Yvette Cedex, France.* [c] *Sorbonne Université, CNRS, MONARIS, UMR 8233, 4 place Jussieu, Paris, F-75005 France*
[d] *Freie Universität Berlin, Institut für Chemie und Biochemie, Fabeckstrasse 34-36, D-14195 Berlin, Germany*
[e] *Manufacture Française des Pneumatiques Michelin, Centre de Technologie de Ladoux – Rue Orange – 63118 – Cébazat*
[f] *University of Chemistry and Technology, Department of Analytical Chemistry, Technická 5, 166 28 Prague 6, Czech Republic*

Proofs to: Dr. Adina CEAUSU-VELCESCU
Université de Perpignan,
LAMPS, 52 Avenue Paul Alduy, 66860 Perpignan Cedex France
Tel. (0033)4 68 66 22 19
E-mail address: adina@univ-perp.fr

Tables: 3

Figures: 4

Keywords: chloroform, high-resolution infrared spectroscopy, excited vibrational states, difference band

Abstract

The ν_4=1 fundamental vibration of chloroform (C-H bending vibration, E symmetry) has been reinvestigated at high-resolution. For this purpose, FTIR spectra recorded in the regions of the ν_4 (1220 cm^{-1}) and $\nu_4 - \nu_3$ (853 cm^{-1}) bands were employed. Spectra were recorded at the Synchrotron Soleil, using a monoisotopic $CH^{35}Cl_3$ sample. More than 6900 transitions were assigned, among which more than 4200 in the difference band. Assignments span the $0 \leq J \leq 100$ and $-75 \leq K''\Delta K \leq 75$ values, despite the systematic overlaps of transitions, observed over a wide range of the spectrum. These overlaps, giving rise to remarkable clustering effects, are characteristic of both the fundamental ν_4 and the difference ν_4-ν_3 bands. They are also, sometimes, source of misassignments, especially when the systematic use of the lower state combination differences as a checking is not possible. In this regard, we have to notice here that the indirect assignment checking through fundamental and difference transitions sharing a common upper level allowed us to systematically correct and extend the *K*-assignments of the ${}^{r}R_K(J)$ transitions in the ν_4 band.

In the least-squares fit, the ground state parameters were fixed to the most recent experimental values. The parameters of the ν_3=1 level could be refined and improved with respect to previous determination, thanks to about 800 IR data collected from a FTIR spectrum of the ν_3 band, together with more than 1300 MMW data in the ν_3=1 level ($22 \leq J \leq 98$ and $0 \leq K \leq 79$).

The theoretical model used for the ν_4=1 fundamental vibration is that of an isolated vibrational level, and ten molecular parameters were refined; the global standard deviation of the fit was of 0.160×10^{-3} cm^{-1}, which is of the order of the accuracy of the experimental data.

1. Introduction

The present work is a part of the systematic investigation of the rotational and rovibrational spectra of chloroform. The ν_4 infrared band has been already studied with high-resolution several years ago by Anttila *et al.* [1]. These authors pointed out the strange appearance of this band, with the higher wavenumber side dominated by strong, equally spaced, band heads, whereas the lower wavenumber side presents a dense forest-structure, without any regularity. Despite these difficulties, the authors of Ref. [1] finally assigned more than 2000 rovibrational transitions with ΔK= -1, and about 1000 transitions with ΔK=+1. The results of the least-squares calculations were sought as being generally good, except for the *R* side of the spectrum; indeed, the standard deviation was of 0.8×10^{-3} cm^{-1} for the *R* lines, compared to 0.59×10^{-3} cm^{-1} for the *P* ones. Several hypotheses were proposed in order to explain these discrepancies, among which a $l(2,-1)$ resonance, or the possibility of an accidental resonance with the $\nu_2 + 2\nu_6$ level, near 1196 cm^{-1}. Nevertheless, none of these interactions seemed to give a solution to the problem. Another discrepancy pointed out by the authors of Ref. [1] is that between the η parameters obtained for the v_4=1 level and those previously determined for v_4=2 [2]. For all the above mentioned reasons, a reinvestigation of the v_4=1 vibrational level seemed mandatory. Moreover, we have decided to take advantage of the great wealth of difference bands in the chloroform spectrum, and to use also the $\nu_4 - \nu_3$ band, near 853 cm^{-1}, in order to complete the description of the v_4=1 vibrational level. Eventually, the simultaneous use of three kinds of transitions, pertaining respectively to the ν_3 and ν_4 fundamental bands and the $\nu_4 - \nu_3$ difference band and forming a closed loop, allowed us to check, correct and extend the assignments of the ν_4 band with respect to previous work [1].

2. Experimental details

2.1. Sample preparation

Pure [^{35}Cl] chloroform was prepared by treating commercial iodoform, HCI_3, with a small excess of carefully dried Ag^{35}Cl (from Na^{35}Cl; Oak Ridge; 99.32% ^{35}Cl) in a sealed glass ampoule for several days at 100 °C. The ampoules were then connected to a standard greaseless vacuum line and the volatile products were distilled from the remaining solid and worked-up by repeated fractional condensation in vacuo until the separation of $CH^{35}Cl_3$ from traces of the partly converted, less volatile chloro-iodomethanes ($CH^{35}Cl_xI_{3-x}$, $x < 3$) was essentially complete. The purity of the $CH^{35}Cl_3$ sample thus obtained (about 1 mmol) was checked by its known gas-phase IR spectrum [1, 3]. It contained very small traces of N_2O and

CS_2, which are traced to a residual nitrate contamination of the $Ag^{35}Cl$ precipitate and an impurity of the commercial CHI_3 sample, respectively. The isotopic purity could be assessed by recording high resolution spectra of a natural sample of $CHCl_3$ and of the enriched sample in the far IR, where the isotopic shifts are clear and large for the ν_6 and ν_3 bands (to be published). The $CH^{35}Cl_2{}^{37}Cl$ intensities were about 2.5% of the $CH^{35}Cl_3$ ones, thus confirming an enrichment of about 99% in ^{35}Cl.

2.2. High-resolution infrared spectra

Two infrared high-resolution spectra have been used in the present work, in order to collect rovibrational transitions pertaining to the ν_4 and ν_4-ν_3 bands respectively. A third spectrum recorded in the 367 cm^{-1} region was used in order to collect IR data pertaining to the ν_3 band, as described further. All spectra were recorded on an isotopically pure $CH^{35}Cl_3$ sample, using a Bruker IFS-125HR FTIR spectrometer, at the Synchrotron Soleil (France).

The first spectrum (spectrum A), covering the 1190-1240 cm^{-1} spectral region, was recorded employing Globar, an iris with 1.3mm aperture as a source, a KBr/Ge beamsplitter, a home-made HgCdTe detector with cold aperture and focusing optics [4] and a multipass gas cell. The gas cell was a 1m-base length, modified Horn-Pimentel type, with two roof-top mirrors used to recirculate twice the optical beam. It is developed to provide a relatively small volume (about 18 liters) but yet to be capable of relatively long optical path lengths, which can be set from 12 to 120 m by 12 m increments. The sample pressure was of about 1.2 Pa, measured by an Edwards 10 Torr capacitance gauge. The spectrum was recorded with a 12-m optical pathlength and at room temperature (296K); the spectral resolution was about 0.00105 cm^{-1} and 2570 scans were averaged. The spectrum was calibrated by matching the measured positions of either residual CO_2 or N_2O traces (less than 0.01 Pa) to reference wavenumbers available in HITRAN [5] with a root mean square (RMS) deviation of 1×10^{-4} cm^{-1}. Given the precision of the reference lines, it is safe to state a 3×10^{-4} cm^{-1} wavenumber accuracy.

The second spectrum (spectrum B) covers the 844-868 cm^{-1} spectral region and was recorded using similar conditions, but for a 24-m optical path length and a pressure of 82 Pa. A total of 546 scans were co-added and the spectral resolution was of about 0.00125 cm^{-1}. The wavenumber calibration was done similarly to spectrum A.

The third spectrum (spectrum C) covers the 340-440 cm^{-1} spectral region and was recorded with the cell set to a 84-m optical path length and a pressure of 82 Pa. The Synchrotron radiation was used as a source. A Si/Mylar composite beamsplitter and a 4.2K Si-bolometer with a cold, 700 cm^{-1} lowpass filter used as detector. The spectral resolution was of 0.00125

cm^{-1}. Wavenumber calibration was done using residual H_2O and CS_2 impurity lines with a root mean square (RMS) deviation of 1×10^{-4} cm^{-1}. We thus estimate a 3×10^{-4} cm^{-1} wavenumber accuracy.

3. Rovibrational spectrum

3.1. The ν_4 fundamental band

This fundamental perpendicular band, centered at 1220 cm^{-1} (Fig. 1a), has been already given a detailed description in a previous high-resolution study [1]; its main characteristics will be therefore not recalled. We must however underline that, while our *K*-assignments of the ΔK= -1 subbands fully agree with those of the previous study [1], those of the ΔK= +1 subbands with $K \geq 1$ are shifted by two units (Fig. 2); *J*-assignments of the ${}^{r}R_0$ series are however identical to those of Ref. [1]. The difficulty in assigning the *K* values of the ΔK= +1 subbands mainly comes from the coincidence between each ${}^{r}R_K(J=K+n)$ cluster (which become partially resolved for $n \geq 21$) and the ${}^{p}Q_{K=n+1}$ branch: indeed, the adjacent lines of the ${}^{p}Q_K$ branch coincide with every second line in the ${}^{r}R_K$ cluster. Also, the use of Ground State Combination Differences (GSCD) as a checking of the *K*-assignments is often of no help in such a congested spectrum; nevertheless, we could perform it successfully for $K \cdot \Delta K \geq 10$ and $-36 \leq K \cdot \Delta K \leq -2$.

Simulation is equally a valuable tool in assigning such crowded and collapsed spectra, as already suggested by the authors of Ref. [1]. However, one has to be careful when comparing the experimental and simulated shapes of the ${}^{r}R_K(J=K+n)$ clusters, because of the presence of several, quite intense hot bands in the region of the ν_4 fundamental band. Their intensity and further contribution to the general shape of the spectrum is not negligible, especially in the central part of the spectrum, as will be explained later.

3.2. The ν_4-ν_3 difference band

This difference band, centered at 853 cm^{-1} (Fig. 1b), has already been mentioned in a 1995 paper by Fuβ and Weizbauer [6], but no assignment of its fine rotational structure has been undertaken by these authors. With its lower level ν_3=1 of A_1 symmetry, the difference band shares several common features with the fundamental ν_4 band. For instance, all ${}^{p}P_K$ series start at almost the same wavenumber; this is also true for the ${}^{r}R_K$ series, and it is due to the accidental approximate equality $2(C - B - C\zeta_4) \approx -2B$. However, as can be seen from Fig. 1b, the appearance of the difference band and its intensity distribution are completely different from those of the ν_4 band. Indeed, in the 847-852 cm^{-1} spectral region, about 25

sharp, regularly spaced peaks, showing a clear intensity alternation, appear (Figs. 1b and 3a). A careful inspection revealed that these peaks are in fact unresolved ${}^{r}Q_K$ branches, their particular sharpness being due to an accidental quasi-coincidence between B_4 and B_3; indeed, the corresponding α^B values are very close to each other: $\alpha_3^B = 7.71 \times 10^{-5}$ cm^{-1} and $\alpha_4^B = 6.75 \times 10^{-5}$ cm^{-1}. Due to the negative value of $C - B - C\zeta_4$, the ${}^{r}Q_K$ branches appear on the lower wavenumber side of the band center; the nearest peak from the band center thus corresponds to the ${}^{r}Q_1$ branch. The ${}^{r}Q_0$ branch, strongly affected by the $l(2,2)$ resonance, is much more spread and degraded to lower wavenumbers (Fig. 3a). The starting wavenumber of the ${}^{r}Q_0$ branch allows us to obtain the band origin of the $\nu_4 - \nu_3$ band, 852.875 cm^{-1} (Fig. 3a), which represents a good estimation of the $(\nu_4)_0 - (\nu_3)_0 + (C_4 - B_4 - 2C\zeta_4)$ quantity.

As said previously, the ${}^{p}P_K(K+n)$ lines form clusters for a given value of $n \geq 0$. Each ${}^{p}P_K(K+n)$ cluster is located between two neighbor ${}^{r}Q_{K=n}$ and ${}^{r}Q_{K=n+1}$ unresolved branches (Fig. 3a). These clusters, by which the assignments were started, become progressively resolved into individual lines and are all degraded to lower wavenumbers with increasing K.

On the higher wavenumber side of the spectrum, the ${}^{r}R_K(K+n)$ lines also form clusters for a given n; these clusters are however much spread than the ${}^{p}P_K(K+n)$ clusters, and are all degraded to higher wavenumbers with increasing K. Each ${}^{r}R_K(K+n)$ is by the way almost superimposed on the ${}^{p}Q_{K=n+1}$ branch (Fig. 3b).

The sharp, quite intense ${}^{r}Q_K$ branches of the $\nu_4 - \nu_3$ band are accompanied by less intense, very similar peaks, also showing intensity alternation (Fig. 3a). These peaks, which become broader and partially resolved at lower wavenumbers, are in fact ${}^{r}Q_K$ branches of the, very weak, $\nu_3 + \nu_4 - 2\nu_3$ band. The shift between a given ${}^{r}Q_K$ branch of the $\nu_4 - \nu_3$ band and its counterpart in the $\nu_3 + \nu_4 - 2\nu_3$ band is of about 0.16 cm^{-1}; this gave us the opportunity of obtaining an experimental value for the x_{34} anharmonicity parameter, as described later.

Another curiosity occurring on spectrum B is the presence of a distinct group of sharp peaks at the high wavenumbers limit of the $\nu_4 - \nu_3$ band; these peaks, clearly visible near 863 cm^{-1} (insert of Fig. 1b), are in fact unresolved ${}^{p}Q_K$ branches, $42 \leq K \leq 60$.

In the early stages of this work, the $v_3 = 1$ parameters were all fixed to the most recent values found in the literature [7, 8]. However, in the course of the assignments of the high-K, ΔK=+1 series of the $\nu_4 - \nu_3$ band, it became soon obvious that the C and D_K values of the lower state $v_3 = 1$ had to be corrected. Indeed, systematic negative $obs - calc$ values, increasing with K

in absolute magnitude but almost *J*-independent, were observed for the ${}^{r}R_K$ series of $K \geq 58$ before this correction has been applied. This behavior can be easily explained by the fact that the wavenumber difference between two ΔK=+1 and ΔK= -1 lines sharing a common upper level is roughly given by:

$$ {}^{r}X_{K-2}(J) - {}^{p}X_{K}(J) = 4(C_3 - B_3 - C\zeta_4)(K-1) $$

When high-K ${}^{p}X_K$ transitions are already assigned and included in a preliminary fit, the small error (of the order of 10^{-7} cm^{-1}) affecting C_3 is somehow 'absorbed' into the $C\zeta_4$ Coriolis parameter of the upper state. However, this correction became insufficient when trying to extend the assignments of the ΔK=+1 transitions, and it was thus necessary to refine also the C_3 parameter of the lower v_3=1 state. Further refinement of D_K^3 allowed us assigning and including in the fit very nice ${}^{r}R_K$ series up to K=75. Eventually, all the molecular parameters of the v_3=1 level up to fourth order were refined, thanks to the inclusion of 830 IR wavenumbers assigned from spectrum C, together with 1350 MMW frequencies assigned from a broadband MMW spectrum already used in our previous studies [9, 10].

4. Results and discussion

The matrix elements of the rovibrational Hamiltonian used in the present work are detailed in Appendix A. Least-squares calculations were performed using the SIMFIT program, described in detail in Ref. [11].

The v_4=1 vibrational level (near 1220 cm^{-1}) is separated from the nearest vibrational level, (v_2=1, v_6=2) estimated to lie at 1196 cm^{-1}, by about 24 cm^{-1}. However, the only possible interaction we would have to consider is a, very local, $(\Delta k = \mp 2, \Delta l = \pm 1)$ interaction. This higher-order interaction, originating from the $\mathbf{H}_{42}$ Hamiltonian term, would essentially affect the $K' \cdot l = 45$ to 47 sublevels of v_4=1. Nevertheless, no systematic deviations were observed in the least-squares calculations for the ${}^{r}X_{44\text{-}46}$ transitions (X = P, Q, or R), neither in the ν_4, nor in the $\nu_4 - \nu_3$ band. The rovibrational transitions reaching the v_4=1 vibrational level could therefore be fitted to an isolated-level model (Table 1). The 6995 assigned transitions (see Table 2) were reproduced with a global standard deviation of 0.160×10^{-3} cm^{-1}, which is of the order of the experimental accuracy. In these calculations, the ground state parameters were all constrained to the most recent available values [12]. Our model included only nine refined diagonal parameters (up to quartic centrifugal distortion) and one off-diagonal parameter (q_{22}), compared to a total of sixteen in the work of Anttila *et al.* [1], out of which several are poorly defined.

We have also tried to refine the q_{12} $l(2,-1)$ interaction parameter, but the trial was unsuccessful, as explained below. In fact, among the $(k; l_4 = +1)/(k+1; l_4 = -1)$ pairs of levels which are coupled through a $l(2,-1)$ interaction, only the $(kl_4 = +1, A_+)/(k = 2; l_4 = -1)$ levels cross, near *J*=50. However, no assigned data were available around this crossing, neither in the ${}^{r}X_0$ (*X*=*R*, *P*), nor in the ${}^{p}X_3$ (*X*=*P*, *Q*) series. Several assignments could however be performed beyond *J*=50 in the ${}^{p}R_3$ series, but these, very weak, lines did not contribute significantly to the determination of the q_{12} parameter, which remained poorly defined. Moreover, the least-squares fit gave very satisfactory results, which demonstrate that the other series are not affected by the $l(2,-1)$ interaction.

We have to notice further that we could in principle refine also the sextic centrifugal distortion parameters H_{JK} and H_{KJ}, which were well-defined in the least-squares calculation. Nevertheless, we preferred fixing them to the corresponding ground state values, for two reasons: (i) the differences $H_{JK}^4 - H_{JK}^0$ and $H_{KJ}^4 - H_{KJ}^0$ were statistically not defined; (ii) fixing H_{JK}^4 and H_{KJ}^4 to the corresponding ground state value had no influence on the standard deviation of the fit.

The frequencies/wavenumbers of the assigned rotational/rovibrational transitions as well as their final reproduction are provided as Supplementary Material, which can be found in the online version, at doi: …

Now, a few words should be said concerning the simulation of the shape of the bandheads of the ${}^{r}R_K(J=K+n)$ clusters in the ν_4 band, which was the main tool for assigning the *K* values in Ref. [1], but which lead to *K*-assignments shifted with respect to ours. Indeed, our simulation (of the ν_4 fundamental band, not including hot bands in this spectral region) revealed slight shifts of the bandheads with respect to the experimental ones, for *n*=0 to 2 (Fig. 4). The shift then quickly diminished with increasing *n* and the higher-*n* bandheads were all perfectly reproduced. Also, the structure of the $n \geq 21$ partially resolved clusters was successfully reproduced. The key of the apparent inconsistency between the experimental and simulated bandheads for n = 0 to 2 is the presence of the $\nu_4^{\pm 1} + \nu_6^{\pm 1} - \nu_6^{\pm 1}$ hot band, the ${}^{r}R_K(J=K+n)$ clusters of which are shifted by about $x_{46} + g_{46} - 2C\zeta_6 \approx -0.204$ cm^{-1} with respect to those of the ν_4 band. The shift is thus accidentally close to $2B$, which gives the separation of adjacent ${}^{r}R_K(J=K+n)$ and ${}^{r}R_K(J=K+n+1)$ clusters and hence each *n*+1 cluster of the hot band is superimposed on the corresponding *n* cluster of the fundamental band, especially for low *n*-values. The *n*=0 cluster of the $\nu_4^{\pm 1} + \nu_6^{\pm 1} - \nu_6^{\pm 1}$ hot band is by the way clearly visible at

1220.284 cm^{-1}, whereas that of the $\nu_4^{\pm 1} + \nu_6^{\mp 1} - \nu_6^{\mp 1}$ hot band appears at 1220.167 cm^{-1} (Fig. 4).

It is also interesting to compare certain parameters of the v_4=1 obtained in our work, with previous experimental determinations [1] and also with force field calculations performed at the MP2/TZ2Pf level [13]. For instance, from $C\zeta_4$=0.055 994 574 (68) cm^{-1} and C_4=0.057 145 018 (10) cm^{-1}, we obtain a Coriolis coupling ζ_4=0.979 868 0 (12), which is closer to ζ_4=0.980 59 (3) obtained in Ref. [1] than to the force field value, ζ_4=0.988. One has to notice also the quite good agreement between our ζ_4 value and the prediction given in the high-resolution study of the v_4=2 level by Pietilä *et al.* [14], 0.978 3.

The situation is different for the main $l(2,2)$ interaction parameter: we obtain q_{22}= – 4.339 18 (38)×10^{-5} cm^{-1}, whereas Ref. [1] gives – 4.439 0 (38)×10^{-5} cm^{-1} and the anharmonic force field calculations [13], – 4.327×10^{-5} cm^{-1}. The agreement between our experimental value and its *ab initio* counterpart is thus almost perfect.

Comparison between experimental and *ab initio* values, for some selected parameters among which the vibration-rotation interaction constants, is summarized in Table 3.

Last, the observed shift between the unresolved ^rQ_K branches of $\nu_4 - \nu_3$ and their counterparts in $\nu_3 + \nu_4 - 2\nu_3$, roughly corresponding to the quantity $2x_{33} - x_{34}$, combined to $x_{33} = -0.0595$ cm^{-1} obtained from the analysis of the ν_3 and $2\nu_3 - \nu_3$ bands, allow obtaining $x_{34} = -0.279$ cm^{-1}. This value agrees well with that obtained by Fuβ and Weizbauer [6] from hot bands accompanying the $2\nu_4^0$ overtone band, $x_{34} = -0.25(10)$ cm^{-1}. The discrepancy between our x_{34} value and that obtained by Pietilä *et al.* [14] from the $2\nu_4^0 + \nu_3 - \nu_3$ hot band, −0.168 0 (2) cm^{-1}, is certainly due to a one-unit shift in the *J*-assignments of the hot band clusters. Performing this shift, the $^qP_{15}$ cluster given in Fig. 4 of Ref. [14] becomes $^qP_{14}$ and is shifted with respect to the $^qP_{14}$ cluster of the $2\nu_4^0$ band by $2x_{34} \approx -0.55$ cm^{-1}; this gives $x_{34} \approx -0.275$ cm^{-1}, again in perfect agreement with our value.

5. Conclusion

The present study, dealing with the rovibrational spectrum of $CH^{35}Cl_3$ in the ν_4 and $\nu_4 - \nu_3$ regions, demonstrates, for such a heavy molecule, that a very large amount of information can sometimes be collected from a hot or a difference band. This information is complementary to that directly obtained through a 'cold' band, allowing a complete description of a certain excited vibrational level. The assignment of several thousands of, often very weak,

rovibrational transitions in these bands thus permits a very accurate determination of rotational and centrifugal distortion constants, as well as rovibrational interaction parameters. Moreover, the correct understanding of the hot bands demonstrates once more its usefulness in the experimental determination of the anharmonicity parameters. As a comparison between experimental and *ab initio* parameters appears to be desirable, the recalculation of the anharmonic force field of $CHCl_3$ at a higher level of electronic structure theory will certainly be needed.

Acknowledgments

Support from Synchrotron SOLEIL (projects 9910148 and 99150017) is gratefully acknowledged. Dr. J. Demaison from the University of Lille (France) is also greatly acknowledged for providing some, unpublished, force field calculations.

Appendix A. Definition of the matrix elements of the effective vibration-rotational Hamiltonian

The diagonal matrix elements were defined conventionally as

$$E_{vr}(J,k,l_t) = E_v + B_v J(J+1) + (C_v - B_v)k^2 - D_J^v J^2(J+1)^2 - D_{JK}^v J(J+1)k^2$$
$$-D_K^v k^4 + H_J^v J^3(J+1)^3 + H_{JK}^v J^2(J+1)^2 k^2 + H_{KJ}^v J(J+1)k^4 + H_K^v k^6$$
$$+L_J^v J^4(J+1)^4 + L_{JJK}^v J^3(J+1)^3 k^2 + L_{JK}^v J^2(J+1)^2 k^4 + L_{JKK}^v J(J+1)k^6 + L_K^v k^8$$
$$+\left[-2(C\zeta_t)_v + \eta_{tJ}J(J+1) + \eta_{tK}k^2 + \tau_{tJ}J^2(J+1)^2 + \tau_{tJK}J(J+1)k^2 + \tau_{tK}k^4\right.$$
$$\left.+\sigma_{tJ}J^3(J+1)^3 + \sigma_{tJK}J^2(J+1)^2k^2 + \sigma_{tKJ}J(J+1)k^4 + \sigma_{tK}k^6\right]kl_t \quad \text{(A1)}$$

The following off-diagonal matrix elements were considered

a) l-type operators

$$\left\langle v_t^{l_t\pm2}; J, k\pm2\middle|\mathbf{H}_{22}+\mathbf{H}_{24}+\mathbf{H}_{26}\middle|v_t^{l_t}; J, k\right\rangle$$
$$= [(v_t \mp l_t)(v_t \pm l_t + 2)]^{1/2}\left\{q_{22} + f_{22}^J J(J+1) + f_{22}^K[k^2 + (k\pm2)^2]\right.$$
$$\left.+f_{22}^{JJ}J^2(J+1)^2 + f_{22}^{JK}J(J+1)[k^2+(k\pm2)^2] + f_{22}^{KK}[k^4+(k\pm2)^4]\right\}F_2^{\pm}(J,k) \quad \text{(A2)}$$

$$\left\langle v_t^{l_t\pm2}; J, k\mp1\middle|\mathbf{H}_{22}+\mathbf{H}_{24}\middle|v_t^{l_t}; J, k\right\rangle = [(v_t \mp l_t)(v_t \pm l_t + 2)]^{\frac{1}{2}}$$
$$\times\left\{\left[q_{12} + f_{12}^J J(J+1)\right](2k\mp1) + f_{12}^K[k^3 + (k\mp1)^3]\right\}F_1^{\mp}(J,k) \quad \text{(A3)}$$

$$\left\langle v_t^{l_t\pm2}; J, k\mp1\middle|\mathbf{H}_{41}+\mathbf{H}_{43}\middle|v_t^{l_t}; J, k\right\rangle = [(v_t \mp l_t)(v_t \pm l_t + 2)]^{\frac{1}{2}}$$
$$\times\left\{q_{12}^l + f_{12}^{lJ}J(J+1) + f_{12}^{lK}[k^2 + (k\mp1)^2]\right\}(2l_t \pm 2)F_1^{\mp}(J,k) \quad \text{(A4)}$$

$$\left\langle v_t^{l_t\pm2}; J, k\mp4\middle|\mathbf{H}_{24}+\mathbf{H}_{26}\middle|v_t^{l_t}; J, k\right\rangle = [(v_t \mp l_t)(v_t \pm l_t + 2)]^{\frac{1}{2}}$$
$$\times\left\{f_{42} + f_{42}^J J(J+1) + f_{42}^K[k^2 + (k\mp4)^2]\right\}F_4^{\mp}(J,k) \quad \text{(A5)}$$

b) Δk=±3 operator

$$\left\langle v_t^{l_t}; J, k\pm3\middle|\mathbf{H}_{23}+\mathbf{H}_{25}\middle|v_t^{l_t}; J, k\right\rangle = \left\{d_t + d_t^J J(J+1) + d_t^K[k^2 + (k\pm3)^2]\right\}l_t F_3^{\pm}(J,k) \quad \text{(A6)}$$

c) Δk=±6 operator

$$\left\langle v_t^{l_t}; J, k\pm6\middle|\mathbf{H}_{06}+\mathbf{H}_{08}\middle|v_t^{l_t}; J, k\right\rangle = \left\{h_3 + h_3^J J(J+1) + h_3^K[k^2 + (k\pm6)^2]\right\}F_6^{\pm}(J,k) \quad \text{(A7)}$$

The notation of the matrix elements of the rotational shifting operators was taken as

$$F_n^{\pm}(J,k) = \prod_{i=1}^{n}[J(J+1) - (k \pm i \mp 1)(k \pm i)]^{1/2} \quad \text{(A8)}$$

Figure captions

Figure 1. (a) Overview spectrum in the region of the ν_4 band (1210-1230 cm^{-1}). Experimental conditions: $CH^{35}Cl_3$ sample; pressure, 1.2 Pa; optical pathlength, 12 m; room temperature. (b) Overview spectrum in the region of the $\nu_4 - \nu_3$ band (845-870 cm^{-1}), with the locations corresponding to subsequent Figures 2 a-b indicated. Insert: detail of the IR spectrum in the 863-865 cm^{-1} region, showing several unresolved ${}^{p}Q_K$ branches of the $\nu_4 - \nu_3$ band, with K assignments indicated. Experimental conditions: $CH^{35}Cl_3$ sample; pressure, 82 Pa; optical pathlength, 24 m; room temperature.

Figure 2. Detail of the IR spectrum in the 1226.56-1226.93 cm^{-1} region, comparing the K-assignments of two adjacent ${}^{r}R_K(J=K+n)$ clusters of the ν_4 band, with n=29 and 30 respectively, in our work (upper panel) and in Ref. [1] (lower panel, reproduced with permission of one of the authors, V.-M. Horneman). Upper panel: experimental conditions as for Fig. 1a; lower panel: $CH^{35}Cl_3$ sample; pressure, 8.4 Pa; optical pathlength, 3.2 m; room temperature.

Figure 3. (a) Detail of the IR spectrum in the 852-853 cm^{-1} region, showing several unresolved ${}^{r}Q_K$ branches of the $\nu_4 - \nu_3$ band, with K assignments indicated. The less intense, unresolved, ${}^{r}Q_K$ branches of the $\nu_4 + \nu_3 - 2\nu_3$ band are marked by an asterisk, and some K assignments are indicated (see text). The assignment combs give the K values within the ${}^{p}P_K(J=K+2)$ and ${}^{p}P_K(J=K+3)$ clusters of the $\nu_4 - \nu_3$ band. (b) Detail of the IR spectrum in the 853-854 cm^{-1} region, showing several partially resolved ${}^{p}Q_K$ branches of the $\nu_4 - \nu_3$ band, with K assignments indicated. The assignment combs give the K values within the ${}^{r}R_K(J=K)$ and ${}^{r}R_K(J=K+1)$ clusters of the $\nu_4 - \nu_3$ band. Experimental conditions as for Figure 1b.

Figure 4. Detail of the infrared spectrum in the 1220.0-1222.0 cm^{-1} region, showing the unresolved ${}^{r}R_K(J=K+n)$ clusters of the ν_4 band, n = 0 to 7. The red trace corresponds to the experimental spectrum, the black one to a synthetic spectrum, which does not include hot bands. The ${}^{r}R_K(J=K+n)$ clusters of several hot bands (n = 0 to 8) are also identified: $\circ = \nu_4^{\pm 1} + \nu_6^{\mp 1} - \nu_6^{\mp 1}$; $* = \nu_4^{\pm 1} + \nu_6^{\pm 1} - \nu_6^{\pm 1}$; $\nabla = \nu_3 + \nu_4^{\pm 1} - \nu_3$.

Table captions

Table 1. Molecular parameters of $CH^{35}Cl_3$ (in cm^{-1}) in the ground, $v_3 = 1$, and $v_4 = 1$ vibrational levels.

Table 2. Data set used in the rovibrational analysis of the $v_4 = 1$ fundamental vibration of $CH^{35}Cl_3$.

Table 3. Computed and experimental parameters in the $v_4 = 1$ vibrational state of $CH^{35}Cl_3$.

References

1 R. Anttila, S. Alanko, V.-M. Horneman, The C-H bending vibration ν_4 of chloroform $CH^{35}Cl_3$, Mol Phys 102; 2004: 1537-42.

2 J. Pietilä, S. Alanko, V.-M. Horneman, R. Anttila, High-resolution infrared studies of ν_1, $2\nu_1$, and $2\nu_4$ bands of $CH^{35}Cl_3$, J Mol Spectrosc 216; 2002: 271-83.

3 J. Pietilä, V.-M. Horneman, R. Anttila, B. Lemoine, F. Reynaud, J.-M. Colmont, The perpendicular fundamental ν_5 of chloroform $^{12}CH^{35}Cl_3$: high resolution infrared study of the ν_5 band together with the millimetre-wave rotational spectrum, Mol Phys 98; 2000: 549-57.

4 M. Faye, M. Bordessoule, B. Kanouté, J.-B. Brubach, P. Roy, L.Manceron, *"Improved mid infrared detector for high spectral or spatial resolution and synchrotron radiation use",* Rev. Sci. Inst. 87; 2016: 063119.

5 Rothman, L.S.; Gordon, I.E.; Barbe, A.; Benner, D.C.; Bernath, P.F.; Birk, M.; Boudon, V.; Brown, L.R.; Campargue, A.; Champion, J.-P.; Chance, K.; Coudert, L.H.; Dana, V.; Devi, V.M.; Fally, S.; Flaud, J.-M.; Gamache, R.R.; Goldman, A.; Jacquemart, D.; Kleiner, I.; Lacome, N.; Lafferty, W.J.; Mandin, J.-Y.; Massie, S.T.; Mikhailenko, S.N.; Miller, C.E.; Moazzen-Ahmadi, N.; Naumenko, O.V.; Nikitin, A.V.; Orphal, J.; Perevalov, V.I.; Perrin, A.; Predoi-Cross, A.; Rinsland, C.P.; Rotger, M.; Simeckova, M.; Smith, M.A.H.; Sung, K.; Tashkun, S.A.; Tennyson, J.; Toth, R.A.; Vandaele, A.C.; Auwera, J.V., The HITRAN 2008 molecular spectroscopic database. J Quant Spectrosc Radiat Transf 110; 2009: 533-72.

6 W. Fuβ and S. Weizbauer, Anharmonische Konstanten von $SiHCl_3$ und $CHCl_3$, Ber. Bunsenges. Phys. Chem. 99; 1995: 289-95.

7 J. Pietilä, V.-M. Horneman, R. Anttila, High-resolution infrared study of the parallel band ν_3 of chloroform $CH^{35}Cl_3$, Mol Phys 96; 1999: 1449-56.

8 L. Margulès, J. Demaison, P. Pracna, Rotational spectrum in the v_6=1 and v_3=1 levels of chloroform, J Mol Struct 795; 2006: 157-62.

9 A. Ceausu-Velcescu, P. Pracna, R. A. Motiyenko, L. Margulès, Rotational spectroscopy in the v_3=v_6=1 and v_6=2 vibrational states of $CH^{35}Cl_3$, J Quant Spectrosc Radiat Transf 250; 2020: 107006.

10 A. Ceausu-Velcescu, P. Pracna, L. Margulès, A. Predoi-Cross, Rotational spectrum of chloroform, "grass-roots among the forest of trees": The v_2 = 1, v_3 = 2, v_5 = 1, and v_6 = 3 vibrational states of $CH^{35}Cl_3$, J Quant Spectrosc Radiat Transf 276; 2021: 107937.

11 P. Pracna, J. Demaison, G. Wlodarczak, A.G. Lesarri, G. Graner, Simultaneous analysis of rovibrational and rotational spectra of the v_5=1 and v_8=1 vibrational levels of propyne, J Mol Spectrosc 177; 1996: 124-33.

12 P. Pracna, A. Ceausu-Velcescu, V.-M. Horneman, The ground and v_6=1 vibrational levels of $HC^{35}Cl_3$: The first high-resolution analysis of the ν_6 fundamental band, J Quant Spectrosc Rad Transf 113; 2012: 1220-5.

13 J. Demaison, private communication.

14 J. Pietilä, S. Alanko, V.-M. Horneman, R. Anttila, High-resolution study infrared studies of ν_1, $2\nu_1$, and $2\nu_4$ bands of $CH^{35}Cl_3$, J Mol Spectrosc 216; 2002: 271-83.

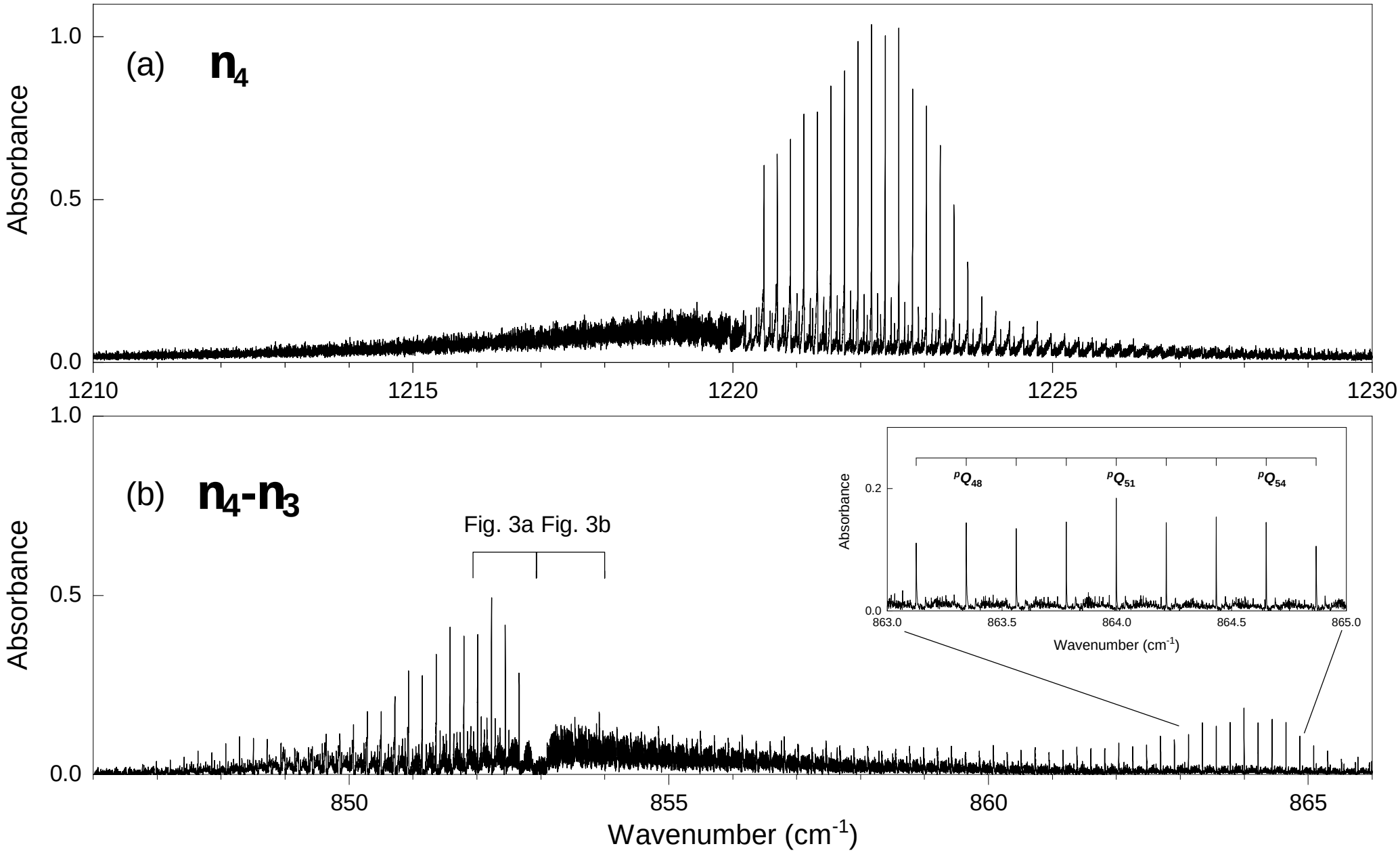
(a) n_4
Absorbance
1.0
0.5
0.0
1210
1215
1220
1225
1230
(b) n_4-n_3
Fig. 3a Fig. 3b
$^pQ_{48}$
$^pQ_{51}$
$^pQ_{54}$
0.2
0.0
863.0
863.5
864.0
864.5
865.0
Wavenumber (cm^{-1})
850
855
860
865
Wavenumber (cm^{-1})

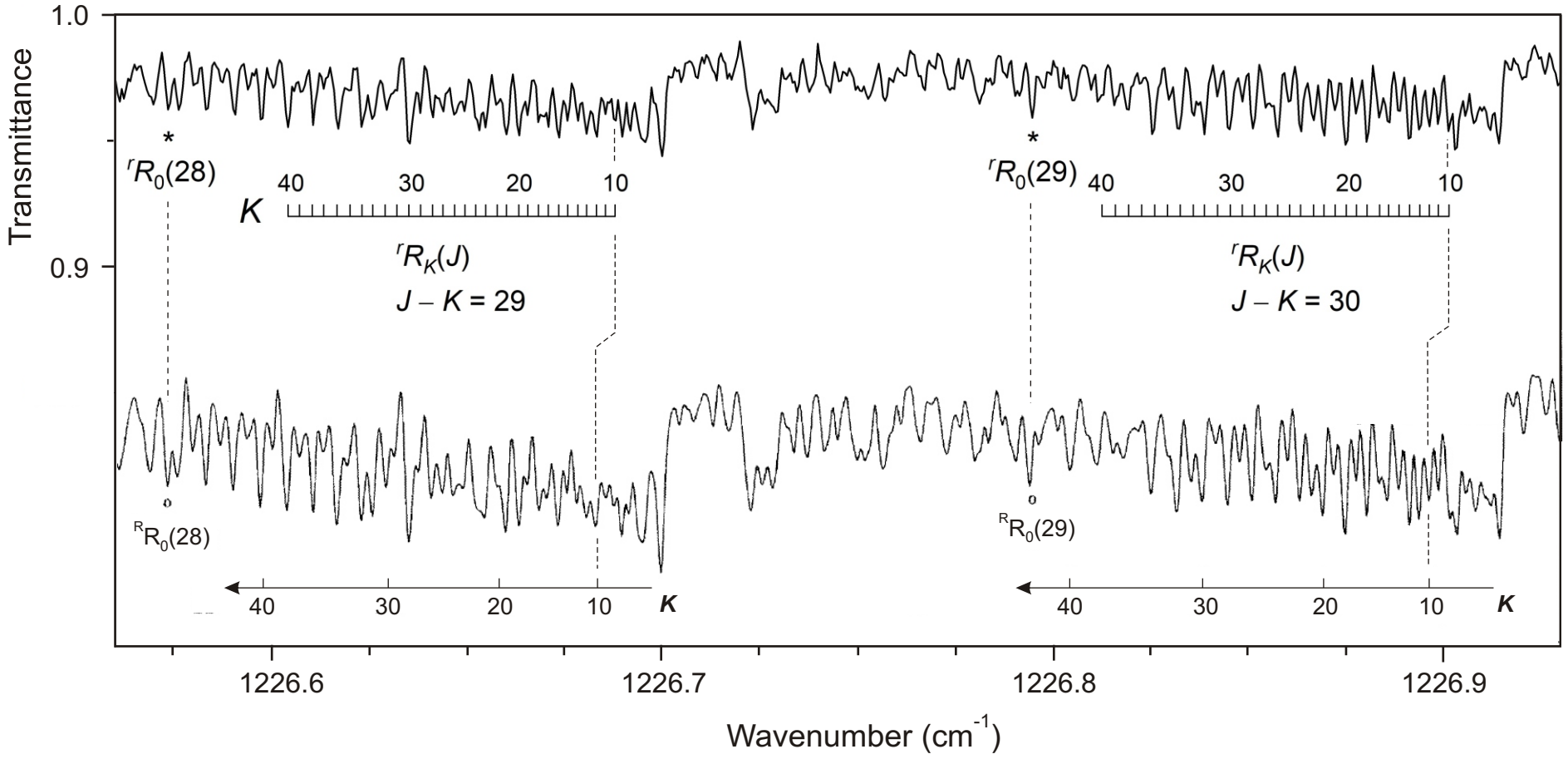
1.0
0.9
Transmittance
*
$^{r}R_0(28)$
K
40
30
20
10
$^{r}R_K(J)$
$J - K = 29$
*
$^{r}R_0(29)$
40
30
20
10
$^{r}R_K(J)$
$J - K = 30$
o
$^{R}R_0(28)$
o
$^{R}R_0(29)$
40
30
20
10
K
40
30
20
10
K
1226.6
1226.7
1226.8
1226.9
Wavenumber (cm^{-1})

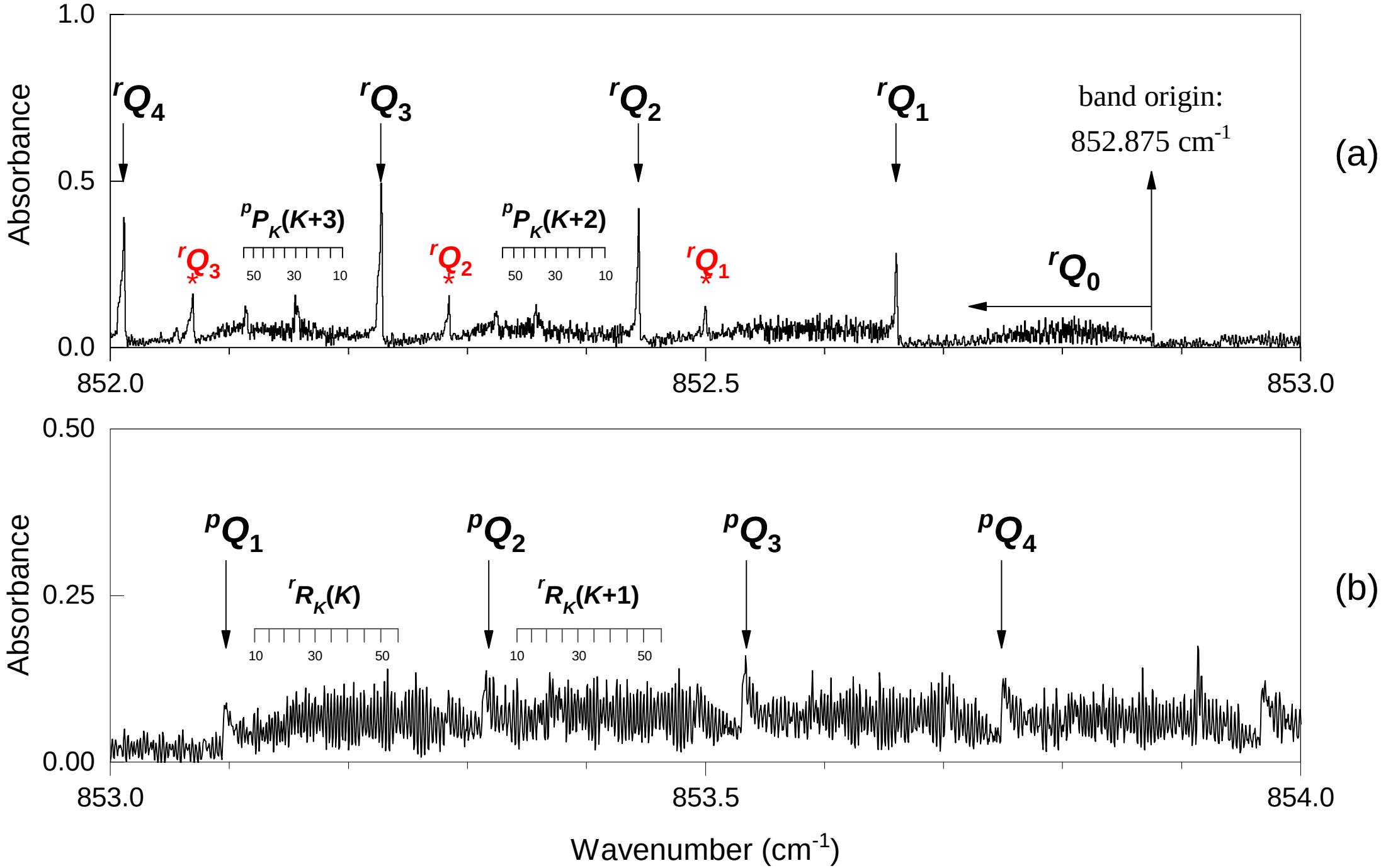
1.0
0.5
0.0
Absorbance
$^{r}Q_4$
$^{r}Q_3$
$^{r}Q_2$
$^{r}Q_1$
band origin:
852.875 cm^{-1}
$^{p}P_K(K+3)$
$^{p}P_K(K+2)$
50 30 10
50 30 10
$^{r}Q_3$*
$^{r}Q_2$*
$^{r}Q_1$*
$^{r}Q_0$
852.0
852.5
853.0
(a)
0.50
0.25
0.00
Absorbance
$^{p}Q_1$
$^{p}Q_2$
$^{p}Q_3$
$^{p}Q_4$
$^{r}R_K(K)$
$^{r}R_K(K+1)$
10 30 50
10 30 50
853.0
853.5
854.0
(b)
Wavenumber (cm^{-1})

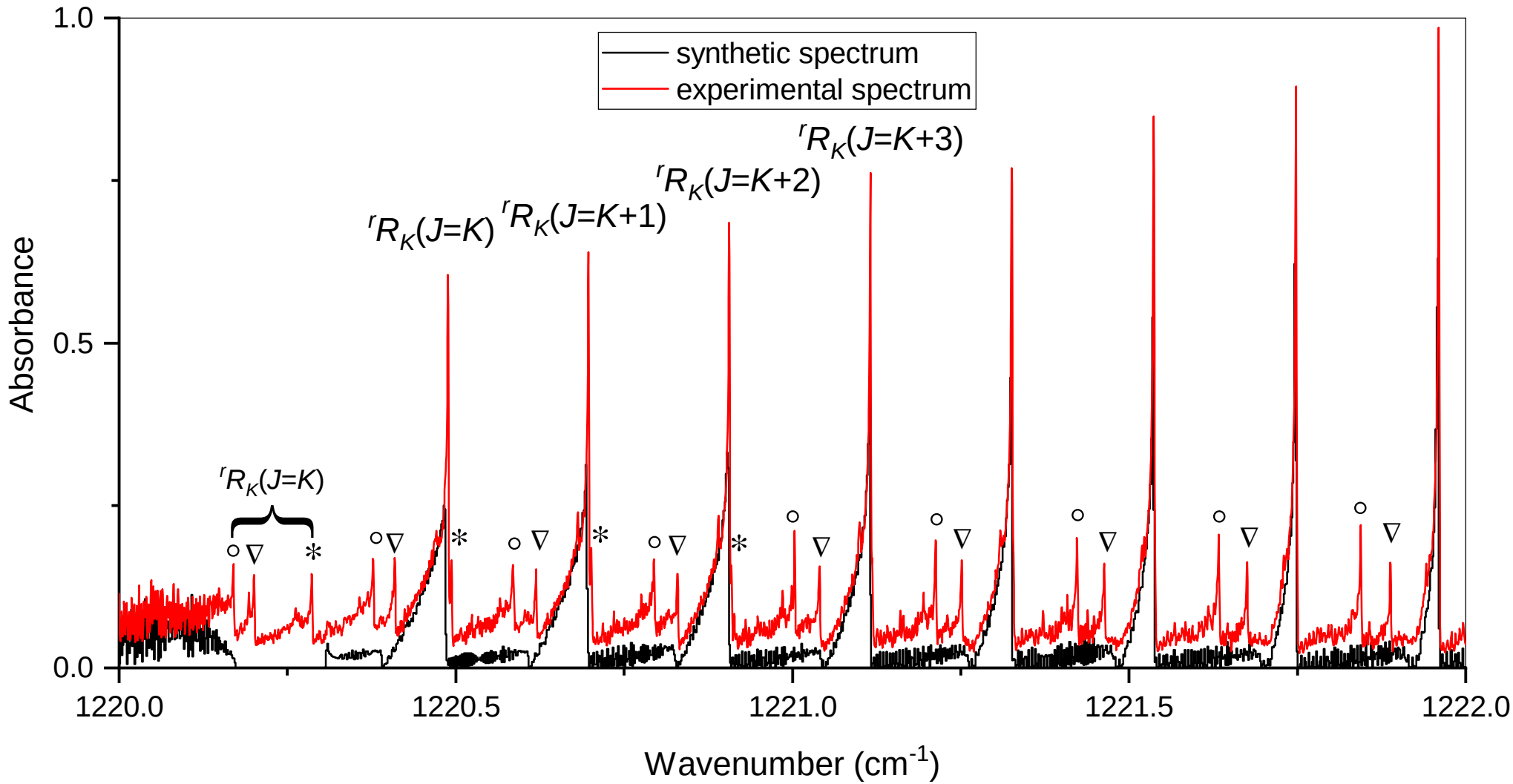
synthetic spectrum
experimental spectrum
$^rR_K(J=K)$
$^rR_K(J=K)$
$^rR_K(J=K+1)$
$^rR_K(J=K+2)$
$^rR_K(J=K+3)$
Absorbance
1.0
0.5
0.0
1220.0
1220.5
1221.0
1221.5
1222.0
Wavenumber (cm^{-1})

Table 1. Molecular parameters of $CH^{35}Cl_3$ (in cm^{-1}) in the ground, $v_3 = 1$, and $v_4 = 1$ vibrational levels

Parameter	Ground state (Ref. [12])	$v_3 = 1$		$v_4 = 1$	
		Present work	Previous works	Present work	Ref. [1]
E		367.295 582 3 (51)	367.295 550 (8)[c]	1220.337 909 5 (60)	1220.338 03 (5)
B	0.110 145 399 6	0.110 068 324 9 (14)	0.110 068 292 8 (48)[d]	0.110 077 925 1 (40)	0.110 076 150 (37)[b]
C	0.057 157 846	0.057 139 244 (11)	0.057 139 250 (11)[c]	0.057 145 018 (10)	0.057 145 48 (17)[b]
$D_J \times 10^8$	5.042 842 06	5.036 758 (28)	5.035 133 (74)[d]	5.051 225 (89)	5.047 33 (58)[b]
$D_{JK} \times 10^8$	-8.398 658	-8.380 20 (15)	-8.381 8 (25)[d]	-8.406 82 (25)	-8.310 (9)[b]
$D_K \times 10^8$	2.754 16	2.743 62 (38)	2.745 95 (15)[c]	2.756 25 (40)	2.392 (10)[b]
$H_J \times 10^{13}$	0.428 18	0.423 83 (17)	0.403 58 (40)[d]	0.428 18[a]	0.428 18[b]
$H_{JK} \times 10^{13}$	-1.670 48	-1.651 7 (10)	-1.647 (10)[d]	-1.670 48[a]	-1.14 (15)[b]
$H_{KJ} \times 10^{13}$	2.126 58	2.108 2 (13)	1.83 (38)[d]	2.126 58[a]	2.126 58[b]
$H_K \times 10^{13}$	-0.827	-0.827[a]		-0.827[a]	-11.17 (26)[b]
$L_J \times 10^{20}$	-8.33	-8.33[a]		-8.33[a]	
$C\zeta$				0.055 994 574 (68)	0.056 036 2 (18)
$\eta_J \times 10^8$				3.308 2 (43)	-6.64 (19)
$\eta_K \times 10^8$				-5.685 0 (60)	29.05 (49)
$\tau_J \times 10^{12}$				0.	6.19 (25)
$\tau_{JK} \times 10^{12}$				0.	4.4 (10)
$\tau_K \times 10^{11}$				0.	-7.7 (17)
$q_{22} \times 10^5$				-4.338 96 (36)	-4.439 0 (38)
$q_{22}^J \times 10^{10}$				0.	0.36 (9)
$h_3 \times 10^{15}$	5.005 8	5.104 4 (83)	5.100 (15)[d]	5.005 8[a]	0.

[a] Constrained to the corresponding GS value.
[b] Calculated from the differences given in Table 3 of Ref. [1] and the corresponding GS parameters.
[c] Ref. [7].
[d] Ref. [8].
Numbers in parentheses are standard deviations in units of the last digit quoted.

Table 2. Data set used in the rovibrational analysis of the $v_4 = 1$ fundamental vibration of $CH^{35}Cl_3$.

Band	Type of transitions	*K* range	J_{max}	Number of data	St. dev. (10^{-3} cm^{-1}/kHz)
ν_4	$\Delta K = +1$	0-66	87	1183	0.162
	$\Delta K = -1$	2-60	83	1516	0.195
$\nu_4 - \nu_3$	$\Delta K = +1$	0-75	104	2693	0.154
	$\Delta K = -1$	1-77	120	1603	0.131
ν_3	IR	3-30	80	830	0.096
	MMW	1-78	98	1350	32.4

Table 3. Computed and experimental parameters in the $v_4 = 1$ vibrational state of $CH^{35}Cl_3$

Parameter	Unit	Experimental	*Ab initio*	% difference
α_4^B	10^{-5} cm^{-1}	6.747 45 (40)	6.45	4.6
α_4^C	10^{-5} cm^{-1}	1.283 2 (10)	1.29	0.5
ζ_4	-	0.979 868 0 (12)	0.988	0.8
q_4	10^{-5} cm^{-1}	-4.338 96 (36)	-4.327	0.3